NASA TECHNICAL NOTE

NASA TN D-6407

c. 1

NASA TN D-6407

COMPUTER-PLOTTER STUDIES OF VIBRATIONAL EFFECTS IN ION-DIPOLE COLLISIONS: "CLASSICAL TUNNELING"

by John V. Dugan, Jr., and R. Bruce Canright, Jr.

Lewis Research Center

Cleveland, Ohio 44135

NATIONAL AERONAUTICS AND SPACE ADMINISTRATION • WASHINGTON, D. C. • JULY 1971

1. Report No. NASA TN D-6407	2. Government Accession No.	3. Recipient's Catalog No.
4. Title and Subtitle COMPUTER-PLOTTER STUDIES OF VIBRATIONAL EFFECTS IN ION-DIPOLE COLLISIONS: "CLASSICAL TUNNELING"		5. Report Date July 1971
		6. Performing Organization Code
7. Author(s) John V. Dugan, Jr., and R. Bruce Canright, Jr.		8. Performing Organization Report No. E-6260
9. Performing Organization Name and Address Lewis Research Center National Aeronautics and Space Administration Cleveland, Ohio 44135		10. Work Unit No. 129-02
		11. Contract or Grant No.
12. Sponsoring Agency Name and Address National Aeronautics and Space Administration Washington, D. C. 20546		13. Type of Report and Period Covered Technical Note
		14. Sponsoring Agency Code
15. Supplementary Notes		

16. Abstract

Computer-plotter studies of ion-dipole collisions are extended to calculating vibrational effects on capture cross sections and formation of ion-molecule complexes. Two different dipole moment variations are assumed about the equilibrium separator of the oscillator. The capture cross section is sensitive to the oscillator model. However, the nature of the ion-molecule complex is relatively insensitive to the oscillator model. In certain collisions, the oscillator becomes constrained so it cannot relax to its equilibrium separation; we choose to call this "classical tunneling." The conditions for tunneling are discussed in terms of collision parameters.

17. Key Words (Suggested by Author(s)) Ion-dipole; Collision complex; Oscillator; "Classical tunneling"; Computer-plotter; Cross section; Vibrational effects		18. Distribution Statement Unclassified - unlimited
19. Security Classif. (of this report) Unclassified	20. Security Classif. (of this page) Unclassified	21. No. of Pages 21 / 22. Price* $3.00

*For sale by the National Technical Information Service, Springfield, Virginia 22151

COMPUTER-PLOTTER STUDIES OF VIBRATIONAL EFFECTS IN ION-DIPOLE COLLISIONS: "CLASSICAL TUNNELING"

by John V. Dugan, Jr., and R. Bruce Canright, Jr.

Lewis Research Center

SUMMARY

Computer-plotter studies of ion-dipole collisions are extended to calculate vibrational effects on capture cross sections and the formation of ion-molecule complexes. Two different dipole moment variations are assumed about the equilibrium separation of the oscillator, one of which best approximates the quantum time average of the dipole moment. The capture cross section is quite sensitive to the Gaussian dipole moment variation $\mu(x)$, being sharply reduced for a $\mu(x)$ which is rapidly varying with oscillator separation. However, the nature of the ion-molecule complex is relatively insensitive to the oscillator model. In certain collisions, the oscillator becomes constrained so it cannot relax to its equilibrium separation; the authors choose to call this "classical tunneling." The probability of this phenomenon is a function of the oscillator constants and the ion-dipole interaction. "Tunneling" conditions are discussed for the two $\mu(x)$ variations in terms of the ratio of the maximum ion-dipole interaction to a "pseudo-oscillator" potential. The latter term depends on the damping constant a (where $\mu = \mu_o \exp^{(-a^2x^2)}$ and μ_o is the "static" dipole moment).

INTRODUCTION

Capture cross sections and collision complex lifetimes have been calculated numerically for ion - polar molecule collisions (refs. 1 to 5). The energy transfer in these collisions has been studied using computer-plotter techniques (refs. 4 and 5). (The polar target molecule is represented by a rotating dipole imbedded in a polarizable sphere. The ion is made to reflect at an intermolecular distance R_c to simulate the hard repulsive cores of the ion and molecule.) Capture cross sections have been calculated to set an upper limit to ion-molecule reaction cross sections and to compare the predicted ion energy dependence with mass spectrometric results (refs. 6 to 8).

The permanent dipole introduces multiple-reflection behavior (ref. 3) corresponding to the formation of long-lived ion-molecule collision complexes. Figure 1 illustrates the mechanism by which multiple reflections occur in terms of a plot of energy against ion-molecule separation. The rotating dipole alters the potential for the outward trajectory, outer turning points are introduced, and multiple reflections occur. For the Langevin case the ion starts in from infinity (where the pair has relative translational energy ϵ), passes over the effective potential barrier at R^*, reflects off the barrier, and returns to large distances. In a simplified case for the dipole target (i.e., the dipole rotates only slightly), the ion passes over the barrier at $R = R'$ before reflection. However, as reflection occurs the dipole can alter its orientation so a new and higher barrier appears at a shifted $R = R''$. The translational energy is now insufficient for the ion to escape, and reflection occurs. This discussion neglects energy transfer to the rotator, which can lower ϵ and cause reflection even for a fixed dipole orientation.

Ion-molecule collision complexes may be of importance as clustering sites in gas discharges or irradiated gases. Such multiple-reflection collisions have calculated lifetimes as large as several hundred times a single-reflection period (ref. 4). Motion pictures have also been made with the computer to study hindered rotation of the dipole by the incident ion (ref. 5). Hindering may favor a specific chemical reaction.

Lifetimes for multiple-reflection collisions have previously been calculated, including rotational and translational degrees of freedom for the ion-molecule collision pair. This report discusses numerical studies of vibrational effects on the capture cross section, the probability of multiple reflections, and collision lifetimes. The vibrational effects are included by approximating the polar target as a rotating oscillator whose dipole moment is a function of internuclear separation along the molecular axis.

EQUATIONS OF MOTION

The equations of motion for the interaction of an ion with a vibrating polar rotator are derived from the Lagrangian

$$L = T_t + T_R + T_v - V_v - V_{int} \tag{1}$$

where T_t is the relative translational energy of the ion-molecule pair, T_R is the rotational energy of the polar molecule, T_v is the kinetic energy of the oscillator, V_v is the potential energy of the oscillator and V_{int} is the ion-molecule interaction term. The first term is the relative energy in the center-of-mass (c.m.) system of ion and molecule and can be written

$$T_t = \frac{m}{2}(\dot{X}^2 + \dot{Y}^2 + \dot{Z}^2) \tag{2}$$

where the ion-molecule separation $R^2 = X^2 + Y^2 + Z^2$ and m is the reduced mass of the ion-molecule pair. The coordinate system is shown in figure 2. The second term is

$$T_R = \frac{I}{2}(\dot{\xi}^2 + \dot{\eta}^2 \sin^2 \xi) \tag{3}$$

for a linear molecule, where I is the moment of inertia. The angles ξ and η are equivalent to polar and azimuthal angles which define the orientation of the negative end of the dipole with respect to a coordinate system fixed on the polar molecule (see fig. 2). The kinetic energy of the oscillator T_v is defined relative to its equilibrium separation r_e via the reduced coordinate x by

$$T_v = \frac{m_o}{2}\dot{x}^2 \tag{4}$$

The coordinate x is $r - r_e$ where r is the instantaneous oscillator separation. Also, m_o is the oscillator reduced mass, which can differ from the mass of the polar molecule. The oscillator potential energy is

$$V_v = \frac{1}{2}k_o x^2 \tag{5}$$

where k_o is the force constant of the oscillator. The ion-molecule interaction potential (refs. 1 to 5) includes the ion-dipole term $-\mu e \cos \gamma/R^2$ and the ion-induced dipole (polarizability) $-\alpha e^2/2R^4$ terms. The angle γ defines the orientation of the vector R with respect to a dipole moment vector $\vec{\mu}$ which has a direction as shown in figure 2. The dipole moment μ equals $\mu_o \exp^{(-a^2x^2)}$, where μ_o is the "static" dipole moment value. It should be noted that the Lagrangian does not include all possible classical electrostatic interactions. The interaction between the opposite charge centers of the dipole is not considered explicitly. However, the electrostatic interaction along the molecular bond is accounted for implicitly by choices of both the force constant k_o and the $\mu(x)$ variation. This is a semiclassical approximation since it says something about the quantum mechanical bonding along the molecular axis. The total interaction potential is

$$V_{int} = \frac{-\mu_o \exp(-a^2x^2) e \cos\gamma}{R^2} - \frac{\alpha e^2}{2R^4} \tag{6}$$

The total Lagrangian in the center-of-mass system is

$$L = \frac{m}{2}(\dot{X}^2 + \dot{Y}^2 + \dot{Z}^2) + \frac{I}{2}(\dot{\xi}^2 + \dot{\eta}^2 \sin^2 \xi) + \frac{1}{2} m_o \dot{x}^2$$

$$- \frac{1}{2} k x_o^2 + \frac{\mu_o \exp(-a^2x^2) e \cos\gamma}{R^2} + \frac{\alpha e^2}{2R^4} \tag{7}$$

where $m\dot{R}_{cm}/2$ (the kinetic energy of the center of mass in the laboratory system) is omitted since $\ddot{R}_{cm} = 0$ and

$$\cos\gamma = \frac{\vec{R} \cdot \vec{\mu}}{R\mu} = \frac{X \sin\xi \sin\eta - Y \sin\xi \cos\eta + Z \cos\xi}{R}$$

The equations of motion are obtained from

$$\frac{d}{dt}\left(\frac{\partial L}{\partial \dot{q}_i}\right) - \left(\frac{\partial L}{\partial q_i}\right) = 0$$

where $q_i = X, Y, Z, \xi, \eta$, and x. These six second-order equations give 12 first-order equations which are solved for the velocities and coordinates employing the variable-step-size Runge-Kutta integration routine described in reference 9.

The equations of motion are

$$\ddot{X} \equiv \dot{V}_X = \left(\frac{\mu e}{mR^5}\right)(R^2 \sin\xi \sin\eta - 3XF_v) - \frac{2\alpha e^2 X}{mR^6} \tag{9}$$

$$\ddot{Y} \equiv \dot{V}_Y = \left(\frac{\mu e}{mR^5}\right)(-R^2 \sin\xi \cos\eta - 3YF_v) - \frac{2\alpha e^2 Y}{mR^6} \tag{10}$$

$$\ddot{Z} \equiv \dot{V}_Z = \left(\frac{\mu e}{mR^5}\right)(R^2 \cos\xi - 3ZF_v) - \frac{2\alpha e^2 Z}{mR^6} \tag{11}$$

with

$$F_V = (X \sin \xi \sin \eta - Y \sin \xi \cos \eta + Z \cos \xi)$$

$$\ddot{\xi} = \dot{\eta}^2 \sin \xi \cos \xi + \left(\frac{\mu e}{IR^3}\right)(-Z \sin \xi + X \cos \xi \sin \eta - Y \cos \xi \cos \eta) \tag{12}$$

$$\ddot{\eta} = \left(\frac{\mu e}{IR^2}\right) \frac{(Y \sin \eta + X \cos \eta) - 2\dot{\eta}\dot{\xi} \cos \xi}{\sin \xi} \tag{13}$$

$$\ddot{x} = -\left(\frac{2a^2 \mu e \cos \gamma}{R^2} + k_o\right) \frac{x}{m_o} \tag{14}$$

MOTION-PICTURE MODEL

Computer-made motion pictures of the oscillator collision were made for collisions between equal mass ions and molecules. Thus, in this case, each particle is equidistant from the center of mass. A sample frame is shown in figure 3. The ion and polar molecule models consist of a positive sign and a dipole, each surrounded by dotted circles of varying radii. The ellipse at the top of the frame indicates the value of x, that is, the difference between the instantaneous oscillator separation and the equilibrium oscillator separation. The motion pictures were used to detect the tunneling phenomenon which is not evident in the time history plots because the x variation is very rapid at small R.

OSCILLATOR MODEL AND INITIAL CONDITIONS

At high frequencies (i.e., on the order of molecular vibrations and fast rotations) the dipole moment of a polar molecule is not constant but is a function of its internuclear separation. The separation of interest is usually that along a particular interatomic bond in the molecule (ref. 10). The variation in dipole moment $\mu(x)$ is assumed Gaussian for these studies (i.e., $\mu = \mu_o \exp^{(-a^2x^2)}$), where μ_o is the "static" dipole moment, a is the damping constant, and x has been defined. The values of μ_o are 3.92 Debye units (1.3×10^{-29} C-m) for CH_3CN and 0.10 Debye units for CO. Such a variation is a reasonably representative approximation for diatomic and polyatomic molecules of interest (ref. 10). (The maximum x value for the free oscillator, set by

values of k_o and initial oscillator energy E_o, was 0.05 Å (0.005 nm) in all cases reported.) To test the sensitivity of the results to the shape of the $\mu(x)$ variation, the damping coefficient a was selected so that μ varied gradually with x for oscillator set A. This a^2 value is 160. For oscillator set B, μ varies more rapidly with x ($\mu = 0.02\ \mu_o$ at $x = \pm 0.05$ Å with $a^2 = 1.6\times10^3$). The shapes of the two Gaussian variations are shown in figure 4.

The most realistic model is that which most nearly simulates the time average of a quantum oscillator (i.e., some $\mu_{eff}(x)$). The $\mu_{eff}(x)$ is the product of $\mu(x)$ weighted by the probability P(x) of finding the oscillator at a given x value. The P(x) is $|\psi^2(x)|$ for a quantum oscillator and this function is sharply Gaussian for a ground-state oscillator (ref. 11). The classical probability P(x) weights the turning points heavily. The quantum and classical probability functions P(x) are shown in figure 5 (ref. 11). The classical time average of $\mu(x)$ with small a^2 is probably a better approximation to the realistic $\mu_{eff}(x)$ for ground-state molecules than $\mu(x)$ with large a^2. In the latter case, small μ values are weighted heavily. The oscillator spends much time at the turning points. These conclusions apply strictly only to a free oscillator. The interaction can change the $\mu_{eff}(x)$ considerably.

The period of change in μ is $\tau_o \approx 2\pi\sqrt{m_o/k_o}$, where k_o and m_o are the oscillator force constant and reduced mass. The values of k_o and m_o for the oscillator define the maximum values of $\dot{x}$ and x, for fixed E_o. The m_o value is roughly the same as the mass of the target molecule and is representative for a diatomic oscillator like CO. The ratio k_o/m_o was chosen so as to reduce computer time; thus, the k_o is somewhat smaller than the value of a representative polar molecule. The energy values E_o chosen were 0.36 eV and 0.036 eV, corresponding to stiff and soft (nearly thermal) oscillators. However, only 50 cases were studied for the stiff oscillators because computer time was prohibitive. A k_o value of 4.8×10^4 dynes per centimeter (0.48 N/cm) was assigned for the calculations reported here, with an m_o value equal to 10 times the mass of the hydrogen atom. These values correspond to a τ_o of $\sim10^{-13}$ second.

Integration for trajectories of all oscillator cases causes extended computer running times, a minimum of 5 minutes for $v = 5\times10^4$ centimeters per second. The oscillation period is only 10^{-2} of the characteristic rotational period τ_R where $\tau_R = \pi\sqrt{2I/E_R}$, E_R is the rotational energy, and I is the moment of inertia. Therefore, a smaller average time step is required to perform the integration. The oscillator motion somewhat separates out from the rotational and translational motion; however, it will be shown that the nature of the $\mu(x)$ variation can be important in determining the ion turning points. Individual collisions with stiff targets require as much as 10 minutes to 1/2 hour computer time, which is clearly prohibitive since hundreds of cases must be studied.

The collision results reported herein are for the soft oscillators with $E_o = 0.036$ eV. The total energy of the free oscillator is

$$E_o = \frac{1}{2} m_o \dot{x}^2 + \frac{1}{2} k_o x^2 \tag{15}$$

where all quantities have been previously defined. The maximum displacement of the free oscillator at large distances from the ion is given by $x_m = \sqrt{2E_o/k_o}$ (i.e., the separation where the oscillator energy is purely potential with no interaction). The initial separations x were chosen randomly in the interval $|x| < x_m$. Approximately 400 collisions have been studied for impact parameters b from 3 to 12 Å. These b values correspond roughly to impact parameters for probable capture with CO and CH_3CN targets (refs. 1 to 3). The oscillator energy remains positive throughout interaction but sometimes decreases in value. Such behavior is, of course, not possible for a quantum oscillator in the ground state, which must have energy $1/2\ h\nu_o$. Thus the observed "cooling" of such oscillators applies only to molecules which are initially in excited vibrational states. The classical oscillator approximation is most adequate in describing variations in energy of soft oscillators since quantum gaps are relatively small.

The differential equation of motion for the oscillator is

$$\ddot{x} = -\left(\frac{2a^2 \mu e \cos \gamma}{R^2} + k_o\right) \frac{x}{m_o} \tag{14}$$

The first term is the ion-dipole interaction term, whereas the second term is the conventional restoring force term for the oscillator.

RESULTS

Multiple-Reflection Behavior

The probability of multiple reflection f_R is the ratio of the number of multiple-reflection collisions to the total number of collisions studied for a constant impact parameter. This probability for oscillating polar targets f_R' is compared with results for purely rotating targets in table I. These results are for an initial ion velocity of 5×10^4 centimeters per second, 25 cases per point. In addition to choosing the initial value of x randomly, the values of initial positions and energies are chosen randomly

(ref. 9). The results of set A are for an a^2 value of 160 which makes $\mu = 2\mu_0/3$ at x_m. Results are presented for both CO and CH_3CN. Results for set B are for an a^2 value of 1.6×10^3 Å^{-2} which makes $\mu = 0.02\ \mu_0$ at $x = \pm0.05$ Å, and include only CH_3CN results. The effect of oscillations clearly depends on impact parameter; however, it is difficult to detect general trends in the results. The variation $\mu(x)$ for the oscillator is important; this can be seen from the difference between identical random number sets for different a^2 values at roughly the same b values. It should be pointed out that although the number of cases studied is limited, the variation between different random number sets of 25 cases (without the oscillator) is roughly 15 percent.

The f_R' value is zero at b = 11 Å because the capture probability for set B drops off abruptly in this range. This dramatic effect on the capture cross section is demonstrated by the plots of capture ratio C_R against the square of the impact parameter b^2 for CH_3CN in figure 6. The capture ratio is the fraction of collisions in which the ion and the molecule approach within a specified separation R (usually several Å). The capture cross section σ_c for ion-dipole collisions is simply related to C_R by $\sigma_c \equiv \pi \int_0^\infty C_R(b)d(b^2)$. There are fewer points for the vibrating targets, only 25 cases per point compared to 50 cases (for the purely rotating targets) because of the prohibitive computer running times. The results agree at low-impact parameters b = 6 and 8 Å. However, there are marked differences between results for b = 10 Å as well as for b = 11 Å. The differences between C_R values are well outside the rough 10 percent variance in cross section between 25- and 50-case sets of trajectories. The oscillator studies were not done for $b > 11$ Å since the C_R value approaches zero. The effect of the oscillator on capture ratio will be much less for CO than for CH_3CN since the polarizability term determines the capture cross section for CO (refs. 4 and 5).

The collision lifetimes are relatively insensitive to vibrations and the average time for multiple-reflection collisions is 2×10^{-11} to 3×10^{-11} second for CH_3CN targets. It should be noted that the trajectories were cut off at a maximum of 10 reflections so that no meaningful maximum reflection time was calculated. Results of previous studies indicate that the average number of reflections is 15 to 25 for certain b values (ref. 5).

Certain features of the energy exchange between the translational, rotational, and vibrational degrees of freedom are shown in the plots of figures 7 and 8. The features of the variations in relative velocity and rotational energy in figure 7 are not affected by the presence of the oscillator. The modulation of the reduced oscillator separation x via the ion-dipole interaction is evident in the region $R \approx 7$ to 8 Å, as shown in figure 8(a) for a CH_3CN target. The corresponding variation in oscillator energy is shown in figure 8(b). The time interval of the modulation envelope is roughly equal to the rotational period.

Multiple-reflection behavior is shown in figure 9(a) for a representative collision. The hindered rotation accompanying multiple reflection is shown in figure 9(b). The symmetrical nature of the net spiraling due to multiple reflections (refs. 2, 3, and 5) is somewhat distorted by the oscillator. However, the general features of this phenomenon are unchanged by the oscillator, as is hindering of the dipole. The hindering of the CH_3CN target occurs at large ion-molecule separations (~7 to 8 Å), as can be seen from the decreasing envelope of the ion-dipole orientation γ plot in figure 9(b). The characteristic ion turning points of the ion-molecule complex are large (10 to 20 Å for CH_3CN) and their values are somewhat insensitive to the presence of the oscillator.

"Classical Tunneling"

Vibrational motion has been added to the ion-dipole motion pictures which were described in references 5 and 12. The modulation of the oscillator which is suggested in the time history plots is confirmed in the motion pictures. This modulation is, of course, dependent on the value of $\cos \gamma$ (i.e., the ion-dipole orientation angle which depends on the relative motion of ion and molecule).

In viewing the motion pictures it was noted that there is a change in the mode of the oscillation in several instances. This change in mode is such that the oscillator cannot relax to its equilibrium position. This behavior is somewhat analogous to quantum mechanical tunneling through a potential barrier so it is herein called "classical tunneling." This change in mode occurs when the oscillator acceleration goes through zero; that is, when the restoring force is balanced by the interaction term. It should be noted that $\ddot{x}$ can be zero where tunneling does not occur (i.e., the free oscillator when $x = 0$).

It is useful to discuss tunneling ($\ddot{x} = 0$) by inspecting the condition that the two terms on the right side of equation (14) cancel, that is,

$$\frac{2a^2 \mu e \cos \gamma}{R^2} + k_o = 0 \tag{16}$$

or rewriting

$$\frac{-\mu_o e \cos \gamma}{R^2} \frac{2a^2}{k_o} \exp^{(-a^2x^2)} = 1 \tag{16a}$$

Taking the natural logarithm of both sides in equation (16a) we obtain the condition

$$\ln\left(\frac{V_m}{V_o}\right) - a^2x^2 = 0 \tag{17}$$

where

$$V_m = \frac{-\mu_o e \cos\gamma}{R^2} \tag{18}$$

and

$$V_o = \frac{k_o}{2a^2} \tag{19}$$

Since a^2x^2 is always positive, it is clear that $\cos\gamma$ must be less than 0 for tunneling to occur. The logarithmic argument is the ratio of the maximum interaction potential V_m to V_o, the latter can be viewed as a pseudo-oscillator potential. Tunneling is clearly quite sensitive to the value of a^2, and the range of a^2x^2 is quite different for the two sets of oscillators. It is useful to inspect the limits on R and rough constraints on γ for tunneling at the most probable a^2x^2 values.

Although $0 \leq a^2x^2 \leq 1.5$ from set A, the mean a^2x^2 value for the nearly free oscillator is approximately equal to 1 since it spends most of its time near the turning points. The condition $(a^2x^2)_{max} = 1.5$ puts an upper limit on R for set A tunneling at 29 Å. At large R where V_m is approximately equal to V_o the tunneling condition suggests $\cos\gamma$ values near -1 for the representative value of a^2x^2. At small R values the ion tends to orient the dipole attractively, thus not meeting the tunneling requirement that $\cos\gamma$ be less than zero.

The range of a^2x^2 values for set B is $0 \leq a^2x^2 \leq 4$; however, the larger values are again favored because of the nature of the weighting function P(x). The upper limit to R for tunneling in this case is only 15 Å. Since relatively large values of V_m/V_o (where $V_o \approx 10^{-1}kT$) are allowable for $R \approx 15$ Å tunneling appears more probable for set B.

The time history plots of oscillator coordinate x and velocity $\dot{x}$ in figure 10 show that $\ddot{x}$ stays near zero for a significant fraction of an oscillation period (where $\dot{x}$ is nearly constant). All tunneling is observed when $\gamma \approx \pi/2$ for set B oscillators (large a^2) so that $\cos\gamma$ is very small and negative. No tunneling is observed for targets from

oscillator set A, but motion pictures were used to detect tunneling in only five cases. It should be pointed out that this phenomenon is less probable than multiple reflection and seems to depend critically on the nature of the dipole moment variation.

CONCLUDING REMARKS

Preliminary studies of vibrational effects on multiple reflections, collision lifetimes, and capture cross sections in ion-dipole collisions have been completed. For thermal oscillators (E_0 = 0.036 eV) the effect of the vibrator depends on impact parameter as well as on target species. The fraction of multiple-reflection cases is a complicated function of the oscillator model, particularly the shape of the dipole moment variation $\mu(x)$. The oscillator can have a dramatic effect on the capture ratio C_R; this corresponds to a lowering of the capture cross section, which is particularly sensitive to the damping constant a. The inclusion of additional degrees of freedom (e.g., coupled oscillators) might markedly increase the collision complex lifetimes. Vibrational studies must be extended to a variation in parameters before more general conclusions can be drawn about the role of the oscillator. "Classical tunneling" of the oscillator via the ion-dipole interaction suggests a mechanism for rearrangement and/or dissociation which operates without the force constant changing. Quantitative conclusions regarding this and related phenomena require further study, particularly in assessing the validity of the semiclassical oscillator model for real polar targets.

Lewis Research Center,
National Aeronautics and Space Administration,
Cleveland, Ohio, April 23, 1971,
129-02.

APPENDIX - SYMBOLS

a	damping constant in dipole moment expression, $Å^{-1}$
b	impact parameter, Å
C_R	capture ratio, dimensionless
E	oscillator energy, eV
e	electronic charge, 1.6×10^{-19} C
f	multiple-reflection fraction dimensionless
k	Planck's constant, 6.623×10^{-34} J-sec
k	oscillator force constant, N m^{-1}
L	Lagrangian, eV
L'	translational angular momentum ($L' = mvb$), kg m^2 sec^{-1}
m	reduced mass of ion-molecule pair, kg
m_o	oscillator mass, kg
R	ion-molecule separation, Å
R_c	ion-molecule reflection distance, Å
R_{cm}	center-of-mass coordinate in laboratory system, Å
R', R''	separations corresponding to maxima in effective potential for ion-dipole interaction, Å
R^*	separation corresponding to maximum in effective potential for Langevin collision, Å
r	instantaneous oscillator separation, Å
r_e	equilibrium oscillator separation, Å
T_R	rotational kinetic energy of polar molecule, eV
T_t	relative translational kinetic energy, eV
T_v	oscillator kinetic energy, eV
V_{int}	interaction potential, eV
V_m	maximum ion-dipole potential, eV
V_o	pseudo-oscillator potential ($V_o = k_o/2a^2$), eV
V_v	oscillator potential energy, eV
X	translational coordinate of ion, Å
x	reduced oscillator separation ($x = r - r_e$), Å
x_m	maximum value of x, Å
Y	translational coordinate of ion, Å
Z	translational coordinate of ion, Å
α	electronic polarizability of polar molecule, Å
β	quantum oscillator coefficient, $Å^{-2}$
γ	ion-dipole orientation angle, deg
ϵ	relative ion-molecule translational energy, eV
η	azimuthal angle for rotational motion, deg
μ	instantaneous value of dipole moment, Debye units (1DU = 3.3×10^{-30} C-m)
μ_o	static value of dipole moment, Debye units

ν_o oscillation frequency, Hz

ξ polar angle for rotational motion, deg

σ_c capture cross section, Å

τ_o period of free oscillation, sec

ω_o oscillation frequency ($\omega_o = 2\pi\nu_o$), rad sec^{-1}

REFERENCES

1. Dugan, John V., Jr.; and Magee, John L.: Capture Collisions Between Ions and Polar Molecules. J. Chem. Phys., vol. 47, no. 9, Nov. 1, 1967, pp. 3103-3112.
2. Dugan, John V., Jr.; Rice, James H.; and Magee, John L.: Calculation of Capture Cross Sections for Ion- Polar-Molecule Collisions Involving Methyl Cyanide. NASA TM X-1586, 1968.
3. Dugan, John V., Jr.; and Rice, James H.: A Computer Plotting Description of Ion-Molecule Collisions with Long-Lived Capture Complexes. NASA TN D-5407, 1969.
4. Dugan, J. V., Jr.; Rice, J. H.; and Magee, J. L.: Evidence for Long-Lived Ion-Molecule Collision Complexes from Numerical Studies. Chem. Phys. Letters, vol. 3, no. 5, May 1969, pp. 323-326.
5. Dugan, John V., Jr.; Canright, R. Bruce, Jr.; and Palmer, Raymond W.: Computer-Made Motion Pictures and Time History Plots of Ion-Polar-Molecule Collisions. NASA TN D-5747, 1970.
6. Theard, Lowell P.; and Hamill, William H.: The Energy Dependence of Cross Sections of Some Ion-Molecule Reactions. Am. Chem. Soc. J., vol. 84, no. 7, Apr. 5, 1962, pp. 1134-1139.
7. Moran, Thomas F.; and Hamill, William H.: Cross Sections of Ion-Permanent-Dipole Reactions by Mass Spectrometry. J. Chem. Phys., vol. 39, no. 6, Sept. 15, 1963, pp. 1413-1422.
8. Dugan, John V., Jr.; and Magee, John L.: Time History Plots and Computer Made Movies of Ion-Polar Molecule Collisions of Interest in Mass Spectrometry. Presented at the American Society of Mass Spectrometry, San Francisco, Calif., June 16-21, 1970.
9. Canright, R. Bruce, Jr.; and Dugan, John V., Jr.: Fortran IV Program for Studying Ion-Polar-Molecule Collisions. NASA TM X-2151, 1971.
10. Herzberg, Gerhard (J. W. T. Spinks, trans.): Vol. 2 of Molecular Spectra and Molecular Structure. Infrared and Raman Spectra of Polyatomic Molecules. D. Van Nostrand Co., Inc., 1945, p. 241.
11. Dicke, Robert H.; and Wittke, James P.: Introduction to Quantum Mechanics. Addison-Wesley Publ. Co., 1960, p. 129.
12. Dugan, John V., Jr.; Palmer, Raymond W.; and Magee, John L.: Computer-Made Movies as a Technique for Studying Ion-Polar Molecule Capture Collisions. Chem. Phys. Letters, vol. 6, no. 3, Aug. 1, 1970, pp. 158-162.

TABLE I. - MULTIPLE-REFLECTION RESULTS FOR

HARMONIC OSCILLATOR STUDY, 25 COLLISIONS

STUDIED PER IMPACT PARAMETER

[Ion velocity, 5×10^{4} cm sec^{-1}; oscillator force constant $k_o = 4.8\times10^{1}$ N m^{-1}; reduced mass of ion-molecule pair $m_o = 1.64\times10^{-26}$ kg.]

Polar molecule	Impact parameter Å(10^{-1} nm)	Fraction of collisions with multiple reflection, f_R		Static dipole moment, μ_o Debye units
		Without oscillator	With oscillator	
Set A (a^2 = 160 $Å^{-2}$)				
CO	3.0	0.24	0.16	0.10
	4.0	.20	.16	.10
	5.0	.24	.16	.10
CH_3CN	5.0	0.24	0.20	3.92
	6.0	.16	.08	↓
	7.0	.36	.48	↓
	9.0	.28	.36	↓
	11.0	.20	.20	↓
Set B ($a^2 = 1.6\times10^{3}$ $Å^{-2}$)				
CH_3CN	6.0	0.16	0.60	3.92
	8.0	.24	.12	↓
	10.0	.24	.32	↓
	11.0	.20	.0	↓

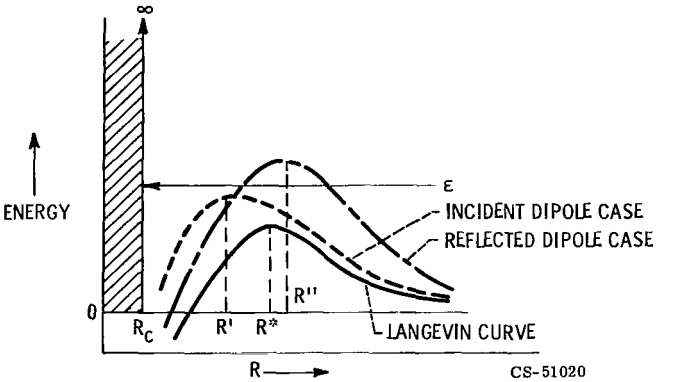

Figure 1. - Schematic diagram illustrating mechanism of multiple-reflection phenomena in ion-dipole collisions with plots of effective potentials for Langevin and permanent dipole collision systems against ion-molecule separation.

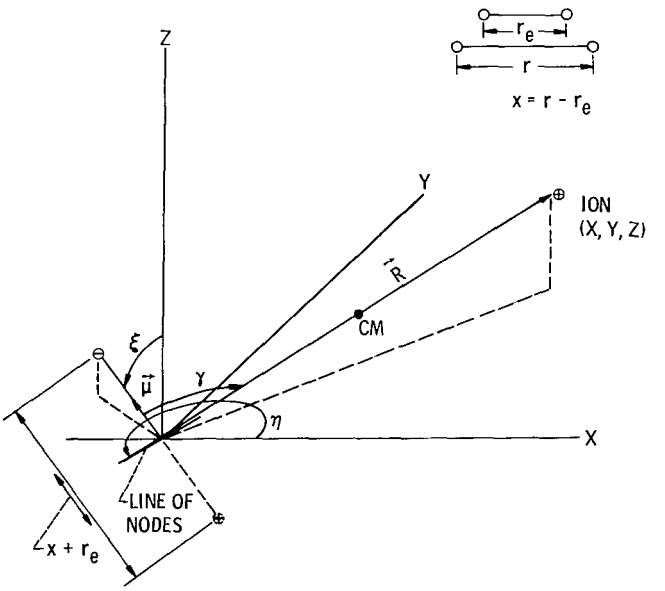

Figure 2. - Coordinate system used for study of ion-dipole interaction with oscillating polar targets.

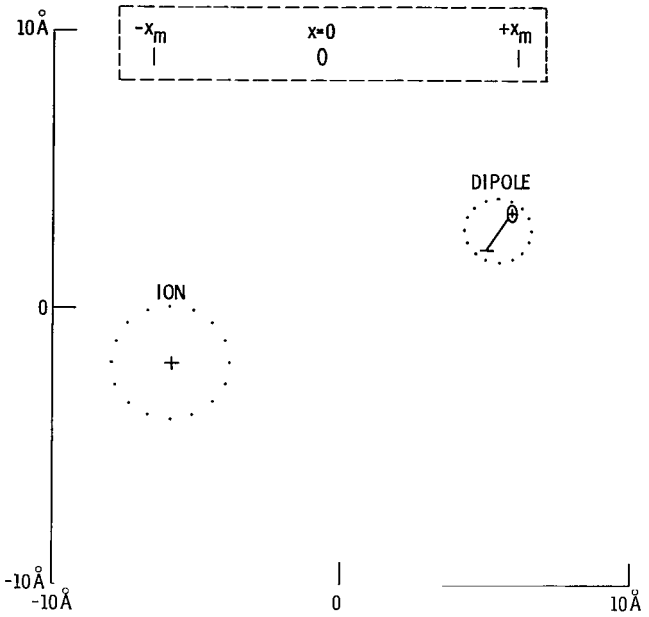

Figure 3. - Sample motion-picture frame for collision study with oscillating targets, showing projections of ion and polar molecule and location of oscillator reduced mass at top of frame. (Oscillator separation scaled by factor of 32 for clarity of display.)

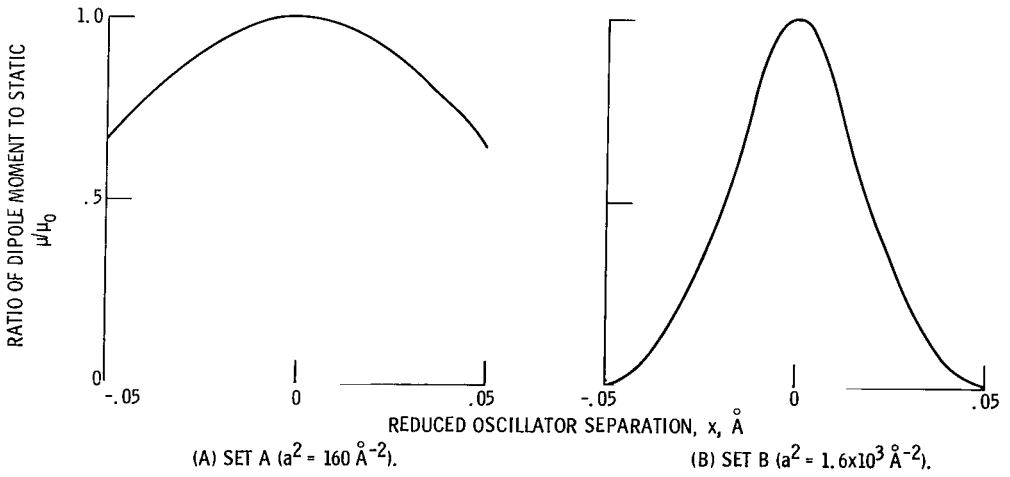

Figure 4. - Dipole moment variation for polar target oscillators studied (sets A and B); $|x_m|_0$ = 0.05 A; $\mu = \mu_0 \exp(-a^2x^2)$.

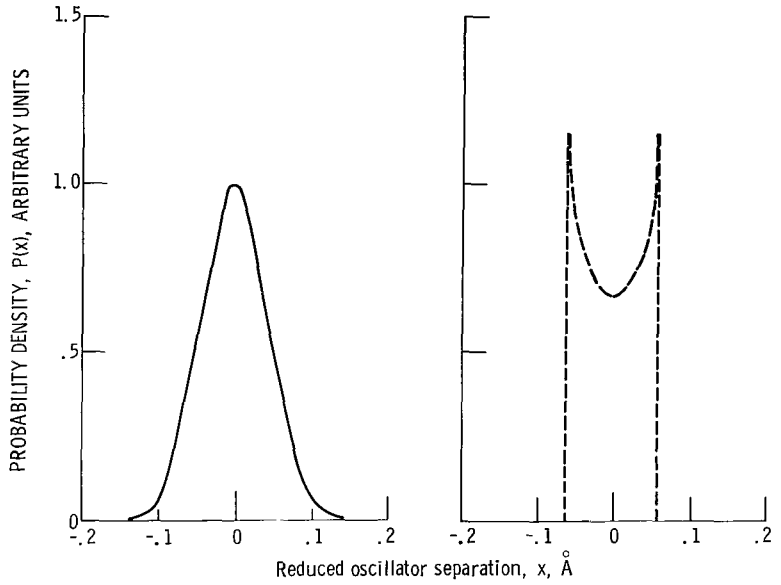

(A) QUANTUM OSCILLATOR; $\psi_0^2 = \sqrt{\beta/\pi}\exp(-\beta x^2)$; $P(x) = \psi_0^2\sqrt{\pi/\beta}$; $\beta = m_0\omega_0/2\hbar$, WHERE ω_0 IS OSCILLATOR FREQUENCY IN RAD SEC^{-1} (REF. 11).

(B) CLASSICAL OSCILLATOR; $P(x) = \left[\pi(2E_0/k_0 - x^2)^{1/2}\right]^{-1}$.

Figure 5. - Comparison of probability densities for quantum and classical ground-state oscillators, as functions of reduced oscillator separation.

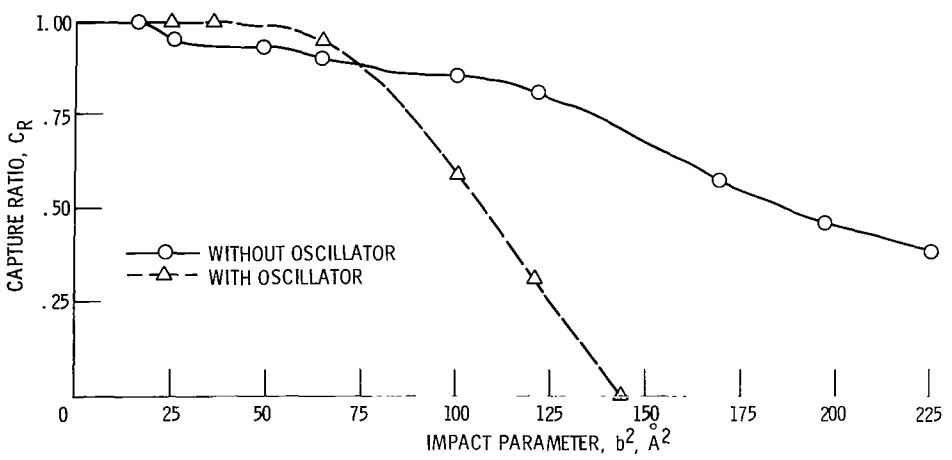

Figure 6. - Comparison of capture ratio variation with impact parameter for oscillating (from set B) and pure rotating polar CH_3CN targets. Results are for initial ion velocity of 5×10^4 cm sec^{-1} where capture cross section $\sigma_c \equiv \pi\int_0^\infty C_R(b^2)d(b^2)$.

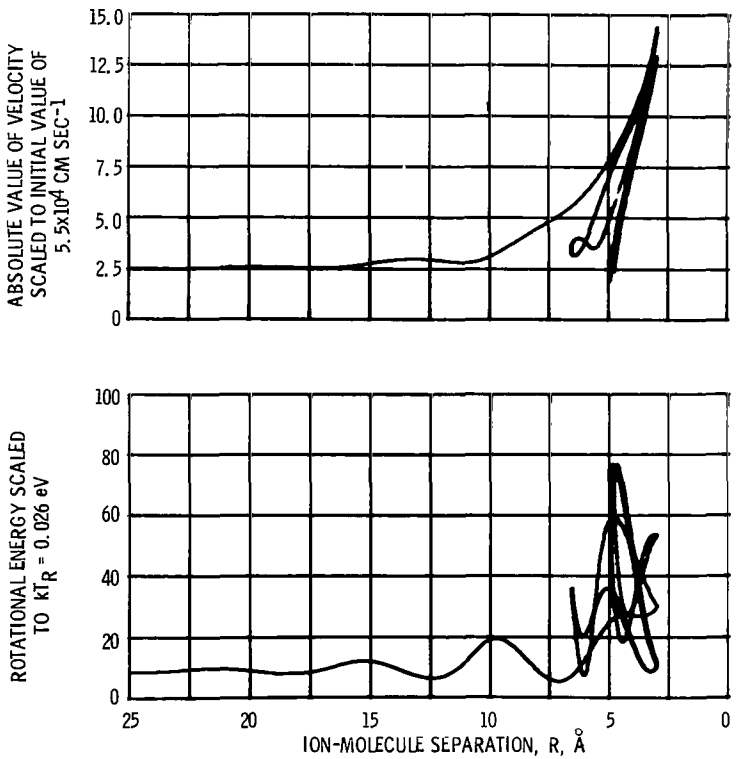

Figure 7. - Variation of relative velocity and polar molecule rotational energy during CH_3CN - parent ion multiple-reflection capture collision with oscillating target.

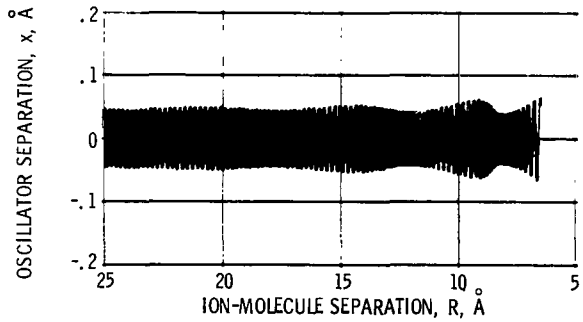

(A) OSCILLATOR SEPARATION.

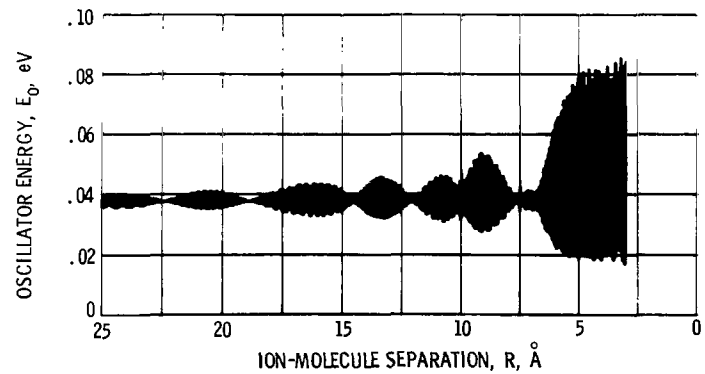

(B) OSCILLATOR ENERGY.

Figure 8. - Variations in oscillator separation and oscillator energy before reflection in CH_3CN - parent ion capture collision with oscillating target from set B ($a^2 = 1.6 \times 10^3$ Å^{-2}).

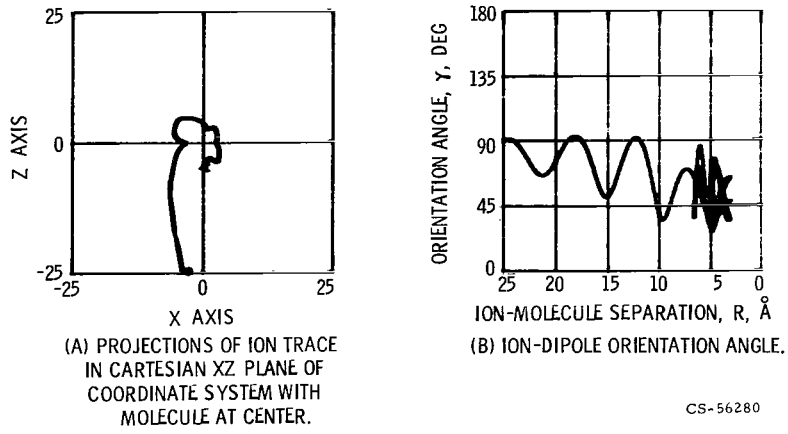

(A) PROJECTIONS OF ION TRACE IN CARTESIAN XZ PLANE OF COORDINATE SYSTEM WITH MOLECULE AT CENTER.

(B) ION-DIPOLE ORIENTATION ANGLE.

Figure 9. - Evidence for multiple reflection and hindered rotation behavior in CH_3CN ion-dipole collisions with oscillating target.

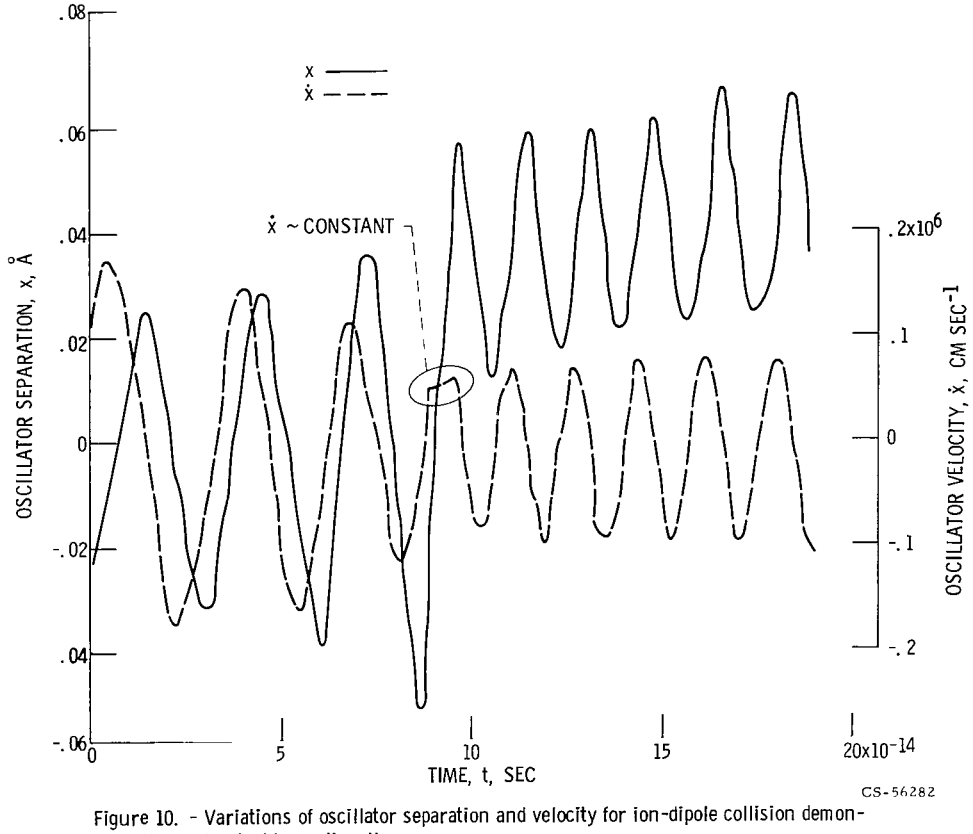

Figure 10. - Variations of oscillator separation and velocity for ion-dipole collision demonstrating "classical tunneling."

NASA-Langley, 1971 —— 24

"The aeronautical and space activities of the United States shall be conducted so as to contribute . . . to the expansion of human knowledge of phenomena in the atmosphere and space. The Administration shall provide for the widest practicable and appropriate dissemination of information concerning its activities and the results thereof."

—NATIONAL AERONAUTICS AND SPACE ACT OF 1958

NASA SCIENTIFIC AND TECHNICAL PUBLICATIONS

TECHNICAL REPORTS: Scientific and technical information considered important, complete, and a lasting contribution to existing knowledge.

TECHNICAL NOTES: Information less broad in scope but nevertheless of importance as a contribution to existing knowledge.

TECHNICAL MEMORANDUMS: Information receiving limited distribution because of preliminary data, security classification, or other reasons.

CONTRACTOR REPORTS: Scientific and technical information generated under a NASA contract or grant and considered an important contribution to existing knowledge.

TECHNICAL TRANSLATIONS: Information published in a foreign language considered to merit NASA distribution in English.

SPECIAL PUBLICATIONS: Information derived from or of value to NASA activities. Publications include conference proceedings, monographs, data compilations, handbooks, sourcebooks, and special bibliographies.

TECHNOLOGY UTILIZATION PUBLICATIONS: Information on technology used by NASA that may be of particular interest in commercial and other non-aerospace applications. Publications include Tech Briefs, Technology Utilization Reports and Technology Surveys.

Details on the availability of these publications may be obtained from:

SCIENTIFIC AND TECHNICAL INFORMATION OFFICE

NATIONAL AERONAUTICS AND SPACE ADMINISTRATION

Washington, D.C. 20546